Proc. Natl. Acad. Sci. USA
Vol. 96, pp. 4449–4454, April 1999
Cell Biology

Mice that lack the angiogenesis inhibitor, thrombospondin 2, mount an altered foreign body reaction characterized by increased vascularity

THEMIS R. KYRIAKIDES*, KATHLEEN J. LEACH†, ALLAN S. HOFFMAN†, BUDDY D. RATNER†‡, AND PAUL BORNSTEIN*§

Departments of *Biochemistry, †Bioengineering, and ‡Chemical Engineering, University of Washington, Seattle, WA 98195

Edited by Robert Langer, Massachusetts Institute of Technology, Cambridge, MA, and approved February 18, 1999 (received for review October 29, 1998)

ABSTRACT **Disruption of the thrombospondin 2 gene (*Thbs2*) in mice results in a complex phenotype characterized chiefly by abnormalities in fibroblasts, connective tissues, and blood vessels. Consideration of this phenotype suggested to us that the foreign body reaction (FBR) might be altered in thrombospondin 2 (TSP2)-null mice. To investigate the participation of TSP2 in the FBR, polydimethylsiloxane (PDMS) and oxidized PDMS (ox-PDMS) disks were implanted in TSP2-null and control mice. Growth of TSP2-null and control skin fibroblasts *in vitro* also was evaluated on both types of disks. Normal fibroblasts grew as a monolayer on both surfaces, but attachment of the cells to ox-PDMS was weak and sensitive to movement. TSP2-null fibroblasts grew as aggregates on both surfaces, and their attachment was further compromised on ox-PDMS. After a 4-week implantation period, both types of PDMS elicited a similar FBR with a collagenous capsule in both TSP2-null and control mice. However, strikingly, the collagenous capsule that formed in TSP2-null mice was highly vascularized and thicker than that formed in normal mice. In addition, abnormally shaped collagen fibers were observed in capsules from mutant mice. These observations indicate that the presence or absence of an extracellular matrix component, TSP2, can influence the nature of the FBR, in particular its vascularity. The expression of TSP2 therefore could represent a molecular target for local inhibitory measures when vascularization of the tissue surrounding an implanted device is desired.**

Soft tissue implants elicit a host response that normally leads to their encapsulation by an avascular collagenous capsule (1). This multistep process, termed the foreign body reaction (FBR), is characterized by a transient acute inflammatory reaction followed by formation of granulation tissue and fibrosis and is clearly related to the biocompatibility of inert materials. Thus capsule formation has been linked to diminished implant performance, often with subsequent failure (2). Consider, for example, implanted electrodes, drug delivery devices, and breast implants, all of which are compromised by capsule formation. The question of why materials with diverse surface properties elicit the same FBR has troubled investigators for more than two decades (3–5). It is believed that implants acquire a protein coat immediately after implantation, which serves as a stimulus for the development of the FBR (6–10), and it has been suggested that fibrinogen is a critical component of this protein coat (10, 11). Adsorption of proteins can be influenced by the surface properties of the material and may lead to modification of the FBR (3, 12–15). It has been suggested that, if all other properties and conditions are equal, materials with hydrophilic surfaces elicit less of an inflammatory response when compared with materials that have surfaces with hydrophobic properties (16).

Nonporous silicone rubber [comprised of polydimethylsiloxane (PDMS), a silica filler, and a crosslinking agent] is a commonly used biomaterial in implants such as breast prostheses, percutaneous catheters, and hydrocephalus shunts. Nonporous biomaterials do not permit in-growth of connective tissue and vasculature and thus serve as excellent inducers of the FBR. The FBR to PDMS or silicone rubber is characterized by the formation of a collagenous capsule that can contract, often with undesirable effects on implants such as mammary prostheses (17). In its native state, PDMS is hydrophobic because of the sheath of methyl groups surrounding the -Si-O- backbone. Treatment of PDMS with oxygen gas plasma replaces some methyl with hydroxyl groups to produce a surface that is more hydrophilic in nature (18). To simplify, PDMS and oxidized PDMS (ox-PDMS) will be referred to as hydrophobic and hydrophilic, respectively. The geometric shape of an implant, and its microarchitecture, also can influence the FBR (19–21). Thus, in addition to surface chemistry, attention has focused on the engineering of implants to modify the smoothness or porosity of materials.

With the exception of site-specific modification of the FBR, such as the response elicited to materials implanted s.c. versus i.p. (22), little consideration has been given to the possible roles of host factors in this process. To explore the possibility of the presence of host modifiers other than fibrinogen, we analyzed the FBR to PDMS and ox-PDMS implants in control and thrombospondin (TSP) 2-null mice. TSP2 and functionally related matricellular proteins do not subserve primarily structural roles but function contextually as adaptors and modulators of cell-matrix interactions (23). TSP2-null mice display a complex phenotype that includes abnormal collagen fibrillogenesis, defective fibroblast adhesion, and increased vascular density in the dermis and subdermal tissues (24). Because these processes are important components of the FBR, we hypothesized that the collagenous capsule, and the extent of vascularization at the implant site, might be altered in these mice. In addition, both hydrophobic and hydrophilic PDMS disks were examined for their ability to support the attachment and growth of control- and TSP2-null-derived dermal fibroblasts *in vitro*. The results of these experiments substantiate the ability of TSP2 to inhibit angiogenesis *in vivo*. Although measurements of cell adhesion *in vitro* showed substantial

The publication costs of this article were defrayed in part by page charge payment. This article must therefore be hereby marked "*advertisement*" in accordance with 18 U.S.C. §1734 solely to indicate this fact.

PNAS is available online at www.pnas.org.

This paper was submitted directly (Track II) to the *Proceedings* office.
Abbreviations: TSP, thrombospondin; FBR, foreign body reaction; PDMS, polydimethylsiloxane; ox-PDMS, oxidized PDMS; ESCA, electron spectroscopy for chemical analysis.
§To whom reprint requests should be addressed at: Department of Biochemistry, Box 357350, University of Washington, Seattle, WA 98195. e-mail: bornsten@u.washington.edu.

differences between PDMS and ox-PDMS, the two biomaterials elicited a similar FBR.

MATERIALS AND METHODS

Materials. Sheets of PDMS sheeting (Silastic NRV HP, lot HX 085147), cured by platinum-catalyzed hydrosilylation, were obtained from Dow-Corning. FBS was purchased from HyClone; Bodipy 558/568 phalloidin was from Molecular Probes; 4′,6′-diamidino-2-phenylindole (DAPI) was from Sigma; 2,2,2-tribromoethanol (Avertin) was from Aldrich; Z-fix aqueous buffered zinc formalin was from Anatech; and Vector ABC elite kit and Vectashield were from Vector Laboratories.

Preparation of PDMS Disks. An arch punch was used to cut disks of 6 or 15 mm diameter. The disks were cleaned three times by sequential ultrasonication in 1% (vol/vol) Triton X-100 in distilled water, followed by washes in acetone and methanol. The discs were stored in ethanol until use. Oxidation of PDMS was performed by radio frequency glow discharge of oxygen gas under the following conditions: 250 mT, 30 W, and oxygen flow rate 4.0 sccm, for 5 min. All PDMS disks were soaked overnight in endotoxin-free PBS (pH 7.2) before cell culture or implantation.

Surface Analysis. Contact angle analysis was performed with a Rane Hart contact angle goniometer to determine the water wettability of the samples. Samples were prepared by drying under a stream of nitrogen gas. Distilled H_20 was added in 7-μl increments to a final drop size of 35 μl and then withdrawn in 7-μl increments to measure receding contact angles. The equilibrium advancing (Θ_{adv}) and receding (Θ_{rec}) contact angles were measured on at least three samples and the values averaged. All error bars in the figures represent SDs. Electron spectroscopy for chemical analysis (ESCA) was performed on a Surface Science Instrument (SSI) X-probe ESCA instrument to determine the chemical composition of the surfaces of the PDMS and ox-PDMS. An aluminium $K_\alpha 1,2$ monochromatized x-ray source was used to stimulate photoemission. The energy of the emitted electrons was measured with a hemispherical energy analyzer at pass energies ranging from 25 eV (resolution 1) to 150 eV (resolution 4). SSI data analysis software was used to calculate the elemental compositions from the peak areas and to peak fit the high-resolution spectra. An electron flood gun set at 5 eV was used to minimize surface charging of the samples. The binding energy scale was referenced by setting the CH_x peak maximum in the C_{1s} spectrum to 285.0 eV. Typical pressures in the analysis chamber during spectral acquisition were 10^{-9} torr.

Cell Culture and Cytochemistry. Mouse skin fibroblasts, isolated as described (24), were cultured on disks placed in 24-well dishes in DMEM supplemented with 10% FCS at 37°C/5% CO_2, at a density of 1×10^5 cells/ml for 48 h. For cytochemical analysis, the cell culture medium was gently aspirated and replaced with 2% paraformaldehyde in PBS for 30 min at room temperature. The cells then were treated with two washes of PBS (5 min/wash), two washes of 0.05 M glycine in PBS (10 min/wash), and two washes of PBS (5 min/wash). The cells then were blocked with 1% BSA/0.05% Triton X-100 in PBS for 30 min and incubated with 4′,6′-diamidino-2-phenylindole (DAPI) (5 mg/ml) and phalloidin (2 units/ml) for 30 min in the dark at room temperature. After three 5-min washes with PBS, the disks were removed from the wells, placed on glass slides, and mounted with Vectashield (Vector). The disks then were examined with the aid of a Nikon Eclipse 800 microscope, equipped with fluorescence optics.

Implantation of PDMS Disks. Six-millimeter disks, prepared as described above, were implanted in the dorsal region of 3-month-old mice. Eight C57BL/129SvTer (four control and four TSP2-null) sex- and age-matched mice were anesthetized with an injection of Avertin i.p. and shaved to facilitate the incision. The area was swabbed with betadine, and then with 70% ethanol. Incisions were made with scissors, and pockets adjacent to the incision site were created with the aid of a curved forceps. Two disks were implanted s.c. per mouse, and the incision was closed with staples. All instruments were rinsed in endotoxin-free water and sterilized before use. After 4 weeks, the mice were anesthetized as described above, and the PDMS disks were explanted en block.

Histochemical Analysis and Quantitation of the FBR. Explanted disks were fixed in 10% formalin for 24 h and then processed for embedding in paraffin. Eight-micrometer-thick sections were generated and stained with hematoxylin and eosin and Verhoeff-van Gieson stains, as described (25). Vascular density was quantitated by measuring erythrocyte-containing vessels within the collagenous capsule. Capsule thickness was estimated microscopically at six different locations on the capsule with the aid of an ocular micrometer. Results, per treatment, represent measurements on eight implants from four mice.

Immunohistochemistry for TSP2. Immunolocalization of TSP2 on paraffin sections was performed as described (24, 25). Briefly, sections were deparaffinized, hydrated, and blocked with 1% BSA in PBS. After incubations with rabbit anti-TSP2 antibodies and anti-rabbit peroxidase-conjugate, interspersed with three PBS washes (5 min per wash), the slides were developed with the ABC reagent and diaminobenzidine substrate (Vector). Controls included sections treated without anti-TSP2 antibodies and sections treated with preimmune sera. Sections from TSP2-null animals served as a negative control for immunoreactivity of TSP2.

RESULTS

Surface Analysis. Oxygen plasma treatment significantly reduced the advancing contact angle of the biomaterial surface. Before treatment, the advancing contact angle of water (Θ_{adv}) for PDMS was 113 ± 1.6°, and the receding contact angle (Θ_{rec}) was 77 ± 0.9°. For the ox-PDMS samples, Θ_{adv} was 28 ± 2.6°; receding contact angles were unmeasurable for ox-PDMS as the boundary of the droplet remained stationary throughout the removal of the water. ESCA data (Fig. 1) suggest that the decrease in Θ_{adv} is caused by the increase in surface oxygen. High-resolution Si_{2p} scans showed a more highly oxidized Si species after treatment, suggesting that the oxygens are bonded directly to the Si atoms. Only small amounts of oxidized carbon were found in high-resolution C_{1s} scans (<10%). These findings indicate that -CH_3 groups were removed from the PDMS during oxygen plasma treatment.

Fibroblast Attachment and Growth on PDMS Disks. Control skin fibroblasts, plated on 15-mm-diameter PDMS disks, attached and grew as a partially overlapping monolayer (Fig. 2*A*). The same cells plated on ox-PDMS disks also appeared to attach and form a monolayer. However, gentle manipulation of the tissue culture plate or movement of the culture medium during replacement of the medium lead to disruption of the monolayer. The cell sheet detached at several areas of the disk and then was disrupted, forming cellular aggregates. Some cells, after 48 h in culture, appeared spread but did not associate extensively with other cells (Fig. 2*C*). TSP2-null fibroblasts did not form a monolayer on either PDMS (Fig. 2*B*) or ox-PDMS (Fig. 2*D*) disks. On PDMS, the cells appeared to attach but failed to spread efficiently. Instead, they formed aggregates that grew in size with time. TSP2-null fibroblasts, plated on ox-PDMS, grew only as aggregates that were loosely attached to the biomaterial surface. Unless care was taken to minimize agitation, these aggregates detached and floated into the culture medium. This behavior may result from abnormalities in synthesis of cell-surface receptors and metalloproteinases (unpublished observations).

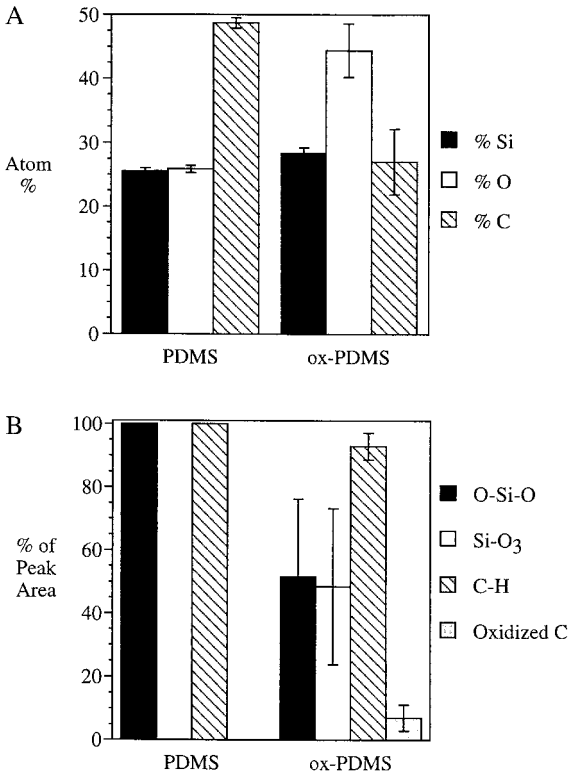

FIG. 1. Characterization of samples by ESCA. (*A*) Elemental composition of the surfaces of unmodified PDMS and oxygen plasma-treated PDMS (ox-PDMS). (*B*) Results from the high-resolution Si_{2p} and C_{1s} spectra ($n = 3$). The % of peak area is the ratio of the area under each of the deconvoluted peaks to the total area under the curve of the element. The error bars indicate SD.

Histological Analysis of the FBR to PDMS and ox-PDMS Disks. After a 4-week implantation period, the disks were removed from anesthetized mice. Superficial examination of the regions surrounding the implants revealed that the FBR was altered in the TSP2-null mice. This change was evidenced by an increase both in the vascularity and in the thickness of the fibrous capsule and connective tissue deposited around the implant. Histological examination of sections showed that collagenous capsules surrounded all implants in both control and TSP2-null mice. Hematoxylin and eosin-stained sections of implanted PDMS are shown for control (Fig. 3*A*) and mutant (Fig. 3*B*) mice. In control mice the FBR to PDMS was characterized by the presence of an avascular capsule with tightly packed collagen fibers and cells (Fig. 3*A*). In TSP2-null mice the capsules surrounding the PDMS disks appeared highly vascularized and contained collagen fibers that were rather loosely packed (Fig. 3*B*). At the lateral edges of the capsules the collagen fibers, stained red with the Verhoeff-van Gieson stain, were highly irregular in shape in the TSP2-null mice (Fig. 3*D*). Collagen fibers in the same area of capsules from control mice appeared more regular in shape and orientation (Fig. 3*C*). No histological differences were observed between the FBR responses to PDMS and ox-PDMS, whether in control or in TSP2-null mice (data not shown).

Quantitation of Parameters of the FBR. The extent of vascularization of collagenous capsules was estimated from sections stained with hematoxylin and eosin. The number of blood vessels and thickness of the capsule that was adjacent to the dermis were greater than the corresponding measurements in the region of the capsule that was adjacent to the panniculus carnosus (data not shown). The data on vascular density are presented in Table 1 and indicate a 5- to 6-fold higher vascularity of foreign body capsules from TSP2-null mice. Table 2 shows the capsule thickness in both control and TSP2-null mice. On average, the capsules formed in the mutant mice were 1½ times thicker than those formed in control mice. This conclusion was reached by measuring capsule thickness at six different capsule locations from a total of eight capsules per genotype. As with the histological analysis, no differences were observed in either vascular density or

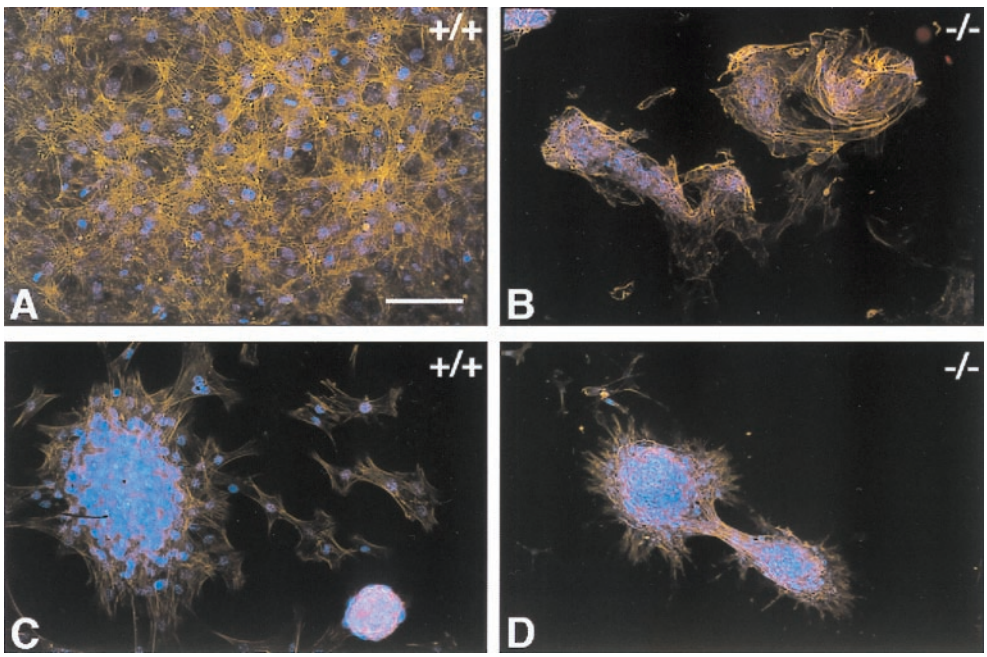

FIG. 2. Mouse skin fibroblasts cultured on silicone rubber disks for 48 h. Control (*A* and *C*) and TSP2-null fibroblasts (*B* and *D*) were plated on PDMS (*A* and *B*) and ox-PDMS (*C* and *D*). Cells were visualized by staining of their actin cytoskeleton with phalloidin (orange) and their nuclei with 4′,6′-diamidino-2-phenylindole (DAPI) (blue). Control fibroblasts formed a confluent overlapping monolayer on PDMS (*A*). On ox-PDMS, the monolayer was loosely attached and was disrupted and reassembled into aggregates during the manipulations associated with culture (*C*). TSP2-null fibroblasts failed to form a monolayer on PDMS (*B*) or on ox-PDMS (*D*) but were associated in aggregates. On ox-PDMS the cellular aggregates tended to slide on the biomaterial surface with movement of the culture medium. (Bar = 50 μm for *A–D*.)

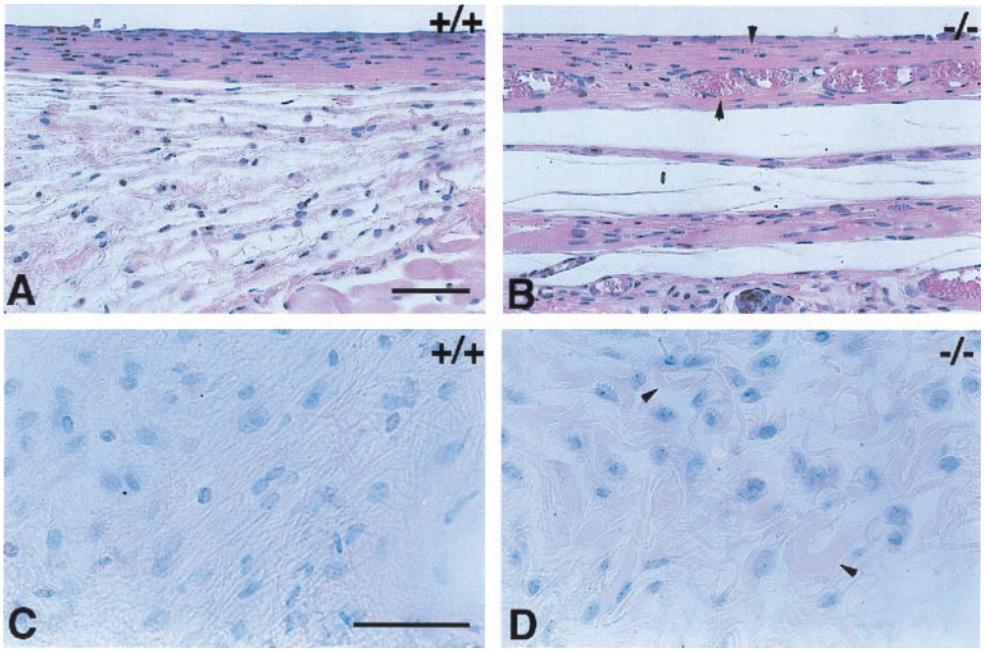

FIG. 3. FBR to implanted PDMS disks. Six-millimeter disks were implanted in control (*A* and *C*) and TSP2-null mice (*B* and *D*) and were removed 4 weeks later. Sections were stained with hematoxylin and eosin (*A* and *B*) or Verhoeff-van Gieson stain (*C* and *D*). Both treatments stain nuclei dark (blue) and cytoplasm and collagen fibers (pink). Capsules forming around the silicone disks were thicker and more highly vascularized (arrowheads) in TSP2-null mice (*B*). Collagen fibers in the capsules of control mice appeared dense, parallel, and organized (*C*). Collagen fibers in the capsules from TSP2-null mice appeared irregular in shape (arrowheads) and were less organized with respect to the implant surface (*D*). (Bars: *A* and *B* = 50 μm; *C* and *D* = 50 μm.)

capsule thickness between the capsules generated by PDMS or ox-PDMS disks, in either control or TSP2-null mice (see Tables 1 and 2).

Immunohistochemical Analysis of the FBR to ox-PDMS. TSP2 was present in the densely packed parallel collagen fibers of the foreign body capsule, as well as in the loose layer of reticular fibers that surrounds it. Immunolocalization for TSP2 showed that the protein was deposited within the capsule at the biomaterial-tissue interface on both sides of the disc, facing the dermis as shown in Fig. 4*A*, and facing the panniculus carnosus and body wall as shown in Fig. 4*B*. Areas of immunoreactivity included the foreign body giant cells at the interface between the implant and the capsule, and cells and matrix within the capsule. It appeared that cells were more immunoreactive than matrix. Cells in the reticular layer were also immunoreactive, but the loose matrix did not appear to stain for TSP2. Capsules and surrounding tissues from TSP2-null mice were not immunoreactive for TSP2 and served as negative controls (Fig. 4 *C* and *D*). Similar results were observed with PDMS implants (data not shown).

DISCUSSION

TSP1, TSP2, and functionally related matricellular proteins such as tenascin-C, osteopontin, and SPARC modulate cell-matrix interactions, in part by either activating or sequestering cytokines and proteases (23, 26). Although preliminary data supported a role for TSP2 as an inhibitor of angiogenesis (27), little was known of its function *in vivo* until the complex phenotype of the TSP2-null mouse was reported. Disruption of the thrombospondin 2 gene (*Thbs2*) in mice leads to disordered fibrillogenesis and fragility in tissues such as skin and tendon, adhesive defects in dermal fibroblasts, and failure to contract collagen gels normally. Increased endosteal bone growth, a bleeding diathesis that can be attributed to a defect in platelet aggregation, and an increase in vascular density in many tissues, including skin and subdermal adipose tissue, are also part of the phenotype (ref. 24 and unpublished observations). The mechanism by which TSP2 influences collagen fibrillogenesis and fibroblast adhesion remains elusive, as indeed is its role in other components of the TSP2-null phenotype, but recent studies of dermal fibroblasts reveal changes in both integrin and metalloproteinase function in TSP2-null cells (Z. Yang, T.R.K., and P.B., unpublished observations).

The combination, in the TSP2-null mouse, of defects in dermal fibroblast function, collagen fibril structure, and vascularity, all of which are important components of the FBR,

Table 1. Neovascularization of capsules

Genotype	Disk	Vessels/capsule*
Thbs2 +/+	PDMS	10 ± 10
	ox-PDMS	12 ± 8
Thbs2 −/−	PDMS	67 ± 13†
	ox-PDMS	60 ± 9†

Disks were implanted s.c. in mice. After a 4-week period, the implants were explanted, and the degree of neovascularization was determined from hematoxylin- and eosin-stained sections. Values shown represent the means ± 1 SD. $n = 8$; four implants per genotype.
*Values corrected for capsule thickness.
†*P* values ≤0.01.

Table 2. Capsule thickness in control and TSP2-null mice

		Capsule thickness facing	
Genotype	Disk	Dermis, μm	Body wall, μm
Thbs2 +/+	PDMS	55 ± 8	24 ± 3
	ox-PDMS	58 ± 7	25 ± 4
Thbs2 −/−	PDMS	91 ± 7*	36 ± 5*
	ox-PDMS	95 ± 8*	38 ± 5*

Disks were explanted 4 weeks after implantation, and sections were stained with hematoxylin and eosin. Capsule thickness was determined with the aid of a microscope micrometer. Values shown represent the means of 16 measurements ±1 SD. A total of eight capsules per genotype were evaluated.
**P* values ≤0.01.

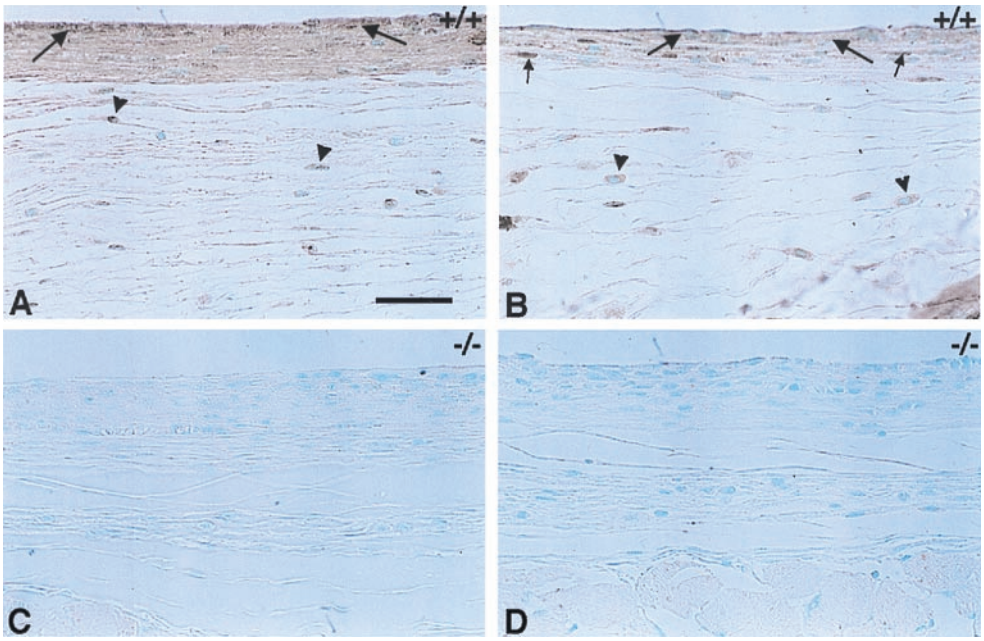

FIG. 4. Immunohistochemical localization of TSP2. TSP2 is present within the foreign body capsules of control animals (*A* and *B*) and is localized to giant cells on the implant-capsule interface (large arrows). TSP2 is also present in the cells and matrix of the capsule (*A* and *B*), with the cells staining more intensely (*B*, small arrows). The loose reticular layer that surrounds the capsule contains fibroblast-like cells that are also positive for TSP2 (*A* and *B*, arrowheads). The presence of TSP2 within the fibers of the reticulum is not obvious. The foreign body capsule is thicker on the side of the implant facing the dermis (*A* and *C*) than on the side facing the body wall (*B* and *D*). TSP2 is absent from the foreign body capsules of TSP2-null mice (*C* and *D*), which serve as a negative control. (Bar = 50 μm for *A–D*.)

suggested to us that this mouse mutant might be informative in studies of implanted biomaterials. PDMS and ox-PDMS disks, implanted s.c. in TSP2-null mice, elicited a FBR that was characterized by the formation of highly vascularized capsules composed of irregularly shaped collagen fibers. The increase in blood vessel density was in the range of 5- to 6-fold, and capsules in mutant animals were 1½ times thicker than control preparations. The presence of TSP2 within the collagenous capsule, both within fibroblasts and possibly as a component of fibrils, was evident by immunohistochemistry. If confirmed by electron microscopy, this finding would constitute the first demonstration of the presence of TSP2 in collagen fibers, because a recent survey of the immunolocation of the protein during murine development failed to detect a clear-cut association with the extracellular matrix (25, 28). These findings strongly support a role for TSP2 as a physiological inhibitor of angiogenesis and suggest that the protein normally functions to inhibit vascularization of the foreign body capsule. In parallel studies in progress, s.c. polyvinyl alcohol sponges, which serve as a model for the early inflammatory and fibroplastic components of the FBR (29), were also more highly vascularized in TSP2-null compared with control mice (T.R.K., Y.-H. Zhu, and P.B., unpublished work).

There is evidence from both endothelial cell migration assays *in vitro* and rodent corneal assays *in vivo* that TSP1 functions as a potent inhibitor of basic fibroblast growth factor-induced angiogenesis (27, 30). Recently, TSP1 also was shown to inhibit angiogenesis and the growth of experimental metastases in mice (31). However, TSP1-null mice display only a mild increase in capillary density in some tissues (26, 32), in contrast to the frank increase in angiogenesis in skin (24) and in foreign body capsule in TSP2-null mice. Because foreign body capsules in TSP2-null mice can be expected to contain normal levels of TSP1, our observations suggest that TSP2 is the more physiologically relevant inhibitor in this system. Comparison of the FBR in TSP1- and TSP2-null mice will be required to confirm this suggestion.

The formation, in the FBR, of an avascular capsule is a protective measure that can be useful to the organism in isolating a noxious material or an infectious focus from the surrounding tissue. However, such isolation would deprive a bioactive implant (e.g., containing cells) of a nutrient supply and could retard the delivery of metabolic products or drugs from implants designed for that purpose. Stabilization of an implant also may be affected because the capsule is rarely adherent to the implant. Under certain circumstances, vascularization of a FBR capsule surrounding an implant has been observed. Woodward (33) has shown that the capsule on the Teflon mesh backing of a silicone breast prosthesis was vascularized, but that the capsule adjacent to the anterior aspect of the prosthesis was not. Picha *et al.* (34) have shown that pillared surface texturing of silicone results in reduced fibrosis and increased vascularization in close proximity to the implant. den Braber *et al.* (35) created microgrooves on silicone rubber implants, thereby increasing the vascularity of the resulting capsules. Karp *et al.* (36) observed the presence of capillaries in capsules that formed around implanted Millipore filters. More recently, in a similar study, Brauker *et al.* (20) showed that vascularization of FBR capsules surrounding membrane filters of varying composition occurred only when pore sizes exceeded 0.8 μm, a size sufficient to permit cellular penetration.

Despite these advances, the current state of knowledge of the mechanisms that determine the response of the host to an implant is inadequate (5, 37). To improve the performance and longevity of implants, factors in the host that modify the FBR should be identified and, if possible, used to advantage. The vascularization of capsules adjacent to PDMS disks that are both nonporous and smooth in TSP2-null mice indicates that foreign body capsules could become vascularized independently of the porosity and surface texture of the implant material, provided the synthesis of endogenous inhibitors of angiogenesis can be inhibited, e.g., by antisense technology, or neutralized, e.g., by specific antibodies. Our observations therefore identify TSP2 as a possible molecular target for improvement of biocompatibility. The FBR also may be less problematic if it is not followed by contraction of the implant capsule, which is a major problem in silicone prosthesis breast

augmentation. The possibility that inhibition of TSP2 will lead to reduced contraction of the capsule is supported by the observation that TSP2-null skin fibroblasts contracted collagen gels poorly in three-dimensional cultures (unpublished observation). In addition, because of their abnormal fibrillar structure, collagen fibers within the capsule may not be able to transmit contractile forces efficiently.

In this study, PDMS and ox-PDMS disks were prepared and evaluated for their ability to support the growth of control and TSP2-null dermal fibroblasts and to elicit a FBR in control and TSP2-null mice. Normal fibroblasts formed monolayers on both surfaces, but attachment of the monolayer to ox-PDMS was compromised. Attachment of TSP2 null fibroblasts was compromised on both surfaces, but more so on ox-PDMS. However, despite the difference in fibroblast attachment on the two types of silicone, no significant differences were observed in the FBR that they elicited when tissues were examined 4 weeks after implantation. The finding that similar FBRs were mounted to PDMS and ox-PDMS in TSP2-null mice suggests that the ability to effectively vascularize foreign body capsules in the absence of TSP2 over-rides the apparently smaller disadvantage of the hydrophobic character of PDMS. The lack of an obvious difference in control mice is consistent with the observation that simple surface modifications do not elicit significant changes in the FBR. However, it is possible that the FBR to the two silicones differs at an earlier stage than was examined in this study or that possible subtle differences were not detected with the relatively small number of mice used in this study.

The present study advances our understanding of the role of TSP2 in the process of angiogenesis and represents an instance in which a modification of the host response significantly increases the vascularity of a foreign body capsule. Our results indicate that TSP2 is critical for inhibition of vascularization of a foreign body capsule, and thus to the generation of a normally avascular capsule, and also suggest measures that could be applied to increase the vascularity of the capsule. Experiments involving other types of nonporous as well as porous biomaterials may reveal whether this regulatory role of TSP2 in implant capsule structure is seen with other relevant implant biomaterials.

We thank Charmaine Harris for technical assistance. The National Science Foundation provided funding for this research through the University of Washington Engineered Biomaterials Engineering Research Center (Grant EEC9529161). This work also was supported by National Institutes of Health Grants HL18645 and DE08229. Surface analysis was partially funded by the National ESCA and Surface Analysis Center for Biomedical Problems (NESAC/BIO) National Institutes of Health Grant RR01296.

1. Williams, D. F. (1989) *J. Biomed. Eng.* **11,** 185–191.
2. Morehead, J. M. & Holt, G. R. (1994) *Otolaryn* **27,** 195–201.
3. Bagnall, R. D. (1977) *J. Biomed. Mater. Res.* **11,** 939–946.
4. Ratner, B. D. (1993) *J. Biomed. Mater. Res.* **27,** 837–850.
5. Ratner, B. D. (1996) *J. Mol. Recogn.* **9,** 617–625.
6. Pitt, W. G., Park, K. & Cooper S. L. (1986) *J. Colloid Interface Sci.* **111,** 343–362.
7. Bohnert, J. L. & Horbett T. A. (1986) *J. Colloid Interface Sci.* **111,** 363–377.
8. Vroman, L., Adams, A. L., Klings, M., Fischer, G. C., Munoz, P. C. & Solensky, R. P. (1977) *Ann. N.Y. Acad. Sci.* **283,** 65–75.
9. Tang, L., Lucas, A. H. & Eaton, J. W. (1993) *G. J. Lab. Clin. Med.* **122,** 292–300.
10. Tang, L. & Eaton, J. W. (1993) *J. Exp. Med.* **178,** 2147–2156.
11. Tang, L., Ugarova, T. P., Plow, E. F. & Eaton, J. W. (1996) *J. Clin. Invest.* **97,** 1329–1334.
12. Seeger, J. M., Ingerno, M. D., Bigatan, E., Klingman, N., Amery, D., Widenhouse, C. & Goldberg, E. P. (1995) *J. Vasc. Surg.* **22,** 327–326.
13. Altankov, G., Grinnell, F. & Groth, T. (1996) *J. Biomed. Mat. Res.* **30,** 385–391.
14. Groth, T. & Altankov, G. (1996) *Biomaterials* **17,** 1227–1234.
15. Kao, W. J., Zhao, Q. H., Hiltner, A. & Anderson, J. M. (1994 *J. Biomed. Mater. Res.* **28**, 73–79.
16. Hunt, J. A., Meijs, G. & Williams, D. F. (1997) *J. Biomed. Mater. Res.* **36,** 542–549.
17. Kasper, C. S. (1994) *Am. J. Clin. Pathol.* **102,** 655–659.
18. Owen, M. J. & Smith, P. J. (1996) in *Polymer Surface Modification*, ed. Mittal, K. L. (VSP, Utrecht, The Netherlands), pp. 3–15.
19. Salthouse, T. E. (1976) *J. Biomed. Mater. Res.* **10,** 197–229.
20. Brauker, J. H., Carr-Brendel, V. E., Martinson, L. A., Crudele, J., Johnston, W. D. & Johnson, R. C. (1995) *J. Biomed. Mater. Res.* **29,** 1517–1524.
21. Smahel, J., Hurwitz, P. J. & Hurwitz, N. (1992) *Plast. Reconstr. Surg.* **92,** 474–479.
22. Benghuzzi, H. (1996) *Biomed. Sci. Instr.* **32,** 81–86.
23. Bornstein, P. (1995) *J. Cell. Biol.* **103,** 231–240.
24. Kyriakides, T. R., Zhu, Y., Smith, L. T., Bain, S. D., Yang, Z., Lin, M. T., Danielson, K. G., Iozzo, R. V., LaMarca, M., McKinney, C. E., *et al*. (1998) *J. Cell. Biol.* **140,** 419–430.
25. Kyriakides, T. R., Zhu, Y., Yang, Z. & Bornstein, P. (1998) *J. Histochem. Cytochem.* **46,** 1–9.
26. Crawford, S. E., Stellmach, V., Murphy-Ullrich, J. E., Ribeiro, S. M. F., Lawler, J., Hynes, R. O., Boivin, G. P. & Bouck, N. (1998) *Cell* **93,** 1159–1170.
27. Volpert, O. V., Tolsma, S. S., Pellerin, S., Feige, J., Chen, H., Mosher, D. F. & Bouck, N. (1995) *Biochem. Biophys. Res. Commun.* **217,** 326–332.
28. Tooney, P. A., Sakai, T., Sakai, K., Aeschlimann, D. & Mosher, D. F. (1998) *Matrix Biol.* **17,** 131–143.
29. Fajardo, L. F., Kowalski, J., Kwan, H. H., Prionas, S. D. & Allison, A. C. (1988) *Lab. Invest.* **58,** 718–724.
30. Tolsma, S. S., Volpert, O. V., Good, D. J., Frazier, W. A., Polverini, P. J. & Bouck, N. (1993) *J. Cell. Biol.* **122,** 497–511.
31. Volpert, O. V., Lawler, J. & Bouck, N. P. (1998) *Proc. Natl. Acad. Sci. USA* **95,** 6343–6348.
32. Lawler, J., Sunday, M., Thibert, V., Duquette, M., George, E. L., Rayburn, H. & Hynes, R. O. (1998*) J. Clin. Invest.* **101**, 982–992.
33. Woodward, S. (1982) *Diabetes Care* **5,** 278–281.
34. Picha, G. J., Drake, R. & Mayhan, K. (1990) *Artificial Organs,* Suppl. 3, **14,** 32–37.
35. den Braber, E. T., Ruijeter, E. de & Jansen, J. A. (1997) *J. Biomed. Mater. Res.* **37,** 539–547.
36. Karp, R. D., Johnson, K. H., Buoen, L. C., Ghobrial, H. K. G., Brand, I. & Brand, K. G. (1973) *J. Nat. Cancer Inst.* **51,** 1275–1285.
37. Tang, L. & Eaton, J. W. (1995) *Am. J. Clin. Pathol.* **103,** 466–471.